

Electronic and magnetic properties of the $(\text{Cr}_{84}\text{Re}_{16})_{100-y}\text{Mn}_y$ alloy system

BS Jacobs¹, AD Faceto^{2,3}, CJ Sheppard¹, ARE Prinsloo¹, PC de Camargo² and AJA de Oliveira²

¹ Department of Physics, University of Johannesburg, PO Box 524, Auckland Park, 2006, South Africa

² Universidade Federal de São Carlos, Rodovia Washington Luís, km 235 - SP-310 São Carlos, São Paulo, Brazil

³ Universidade Federal dos Vales do Jequitinhonha e Mucuri, Avenida Vereador João Narciso, 1380, Unaí, Minas Gerais, Brazil

E-mail address: sjacobs@uj.ac.za

Abstract. This paper reports the results of the temperature dependence of the electrical resistivity (ρ) and magnetic susceptibility (χ) of $(\text{Cr}_{84}\text{Re}_{16})_{100-x}\text{Mn}_x$ alloys with $x = 0.3, 0.4, 0.6, 0.8$ and 3.1 . Anomalies are observed in the $\rho(T)$ curves corresponding to the Néel temperatures (T_N) of the samples. $\chi(T)$ curves of the $(\text{Cr}_{84}\text{Re}_{16})_{100-x}\text{Mn}_x$ alloy system in a constant applied field of 100 Oe was obtained on increasing T after cooling in zero magnetic field (ZFC) and after cooling in a field of 100 Oe (FC). At low temperatures ($T < 10$ K), a sharp increase in χ is observed on increasing T after ZFC. A prominent sharp peak is observed close to 30 K beyond which χ rapidly decreases to lower values. The behaviour of χ is indicative of possible spin glass state at the boundaries of the itinerant antiferromagnetic order established by Mn frozen local moments.

1. Introduction

The magnetic properties of alloys of Cr have been a topic of research for many years, however, without much attention recently. Magnetism of Cr alloys still excites the experimentalist as the unique antiferromagnetic properties of Cr [1] are significantly altered by adding small quantities of other elements. Lomer [2] used the two-band model to explain the Fermi surface of Cr. This model describes the two important features on the Fermi surface of paramagnetic Cr namely the electron “jack” and a slightly larger hole “octahedron”. The shapes of these two Fermi surface features are almost identical and thus shifting of one in reciprocal space through a wave vector (\mathbf{Q}) results in the surfaces “fitting” or “nesting” nearly perfectly against each other [3]. These “connected” electron and hole states condense via Coulombic interaction into a spin-density-wave (SDW) of this wave vector [3]. This leads to the incommensurate (I) SDW magnetic state. The nesting is sensitive to the degree of matching between the two sheets and thus it is expected that the magnetic properties of Cr rely on the topology of the Fermi surface. The Fermi surface topology can be altered by varying the electron distribution [4]. The electron to atom ratio (e/a) of Cr is 6. This can be increased or decreased by alloying with elements to its right or left respectively in the periodic table. Alloying with Mn ($e/a = 7$) results in the increase in size of the electron sheet and decrease in the size of the hole sheet. This makes Cr more commensurate (C) and eventually a CSDW phase is formed. The CSDW state is more

stable than the ISDW phase and the Néel temperature T_N is expected to increase with increase in Mn concentration [4].

The spin glass (SG) state is observed in cases where magnetic impurities (such as Mn or Fe) are hosted in non-magnetic metals [5]. In these systems, below a “freezing (or pinning) transition” at T_P , there is no long range magnetic order but the spins are locked in a frustrated low energy state [6]. The occurrence of the spin glass state in alloys containing Cr and Mn have been reported before [7,8,9,10]. In $\text{Cr}_{1-x}\text{Mn}_x$ alloys, characteristics typical of the spin-glass state, namely hysteresis of $M(H)$, peak in $\chi(T)$ in the ZFC state and relaxation of M as the logarithm of time when H is changed were observed [8]. However, it differs from a conventional SG since the magnetic susceptibility $\chi(T)$ is essentially independent of temperature between T_P and T_N , and that the pinning temperature (T_P) is essentially independent of Mn concentration. In the $(\text{Cr} + 1.5\% \text{ Fe})_{1-x}\text{Mn}_x$ system, the SG state was reported to coexist with Curie-Weiss paramagnetism and at low Mn concentrations ($x \leq 0.3\%$ Mn) the Fe impurity suppresses the spin-glass behaviour [9]. The $\text{Cr}_{80-x}\text{Fe}_{20}\text{Mn}_x$ system displays a sequence of SG-ferromagnetic-antiferromagnetic-paramagnetic magnetic phase transitions on heating from low temperatures [10].

The $\text{Cr}_{84}\text{Re}_{16}$ alloy is in the CSDW state at room temperature [11]. Doping with V (element to the left of Cr in the periodic table) drives the system towards incommensurability and reduces T_N due to the lower electron/atom ratio (e/a) of V [11]. Results of the effect of V doping on this alloy system has been reported [12]. The present study was conducted to understand the nature of the magnetic state when Mn (element to the right of Cr in the periodic table) is used as a dopant. Preliminary investigation confirms the increase of T_N with Mn doping and suggests the presence of the SG state in the $(\text{Cr}_{84}\text{Re}_{16})_{100-x}\text{Mn}_x$ alloy system.

2. Experimental

Ternary $(\text{Cr}_{84}\text{Re}_{16})_{100-y}\text{Mn}_y$ alloys with $y = 0.3, 0.4$ and $0.6, 0.8$ and 3.1 were prepared by repeated arc melting in a purified argon atmosphere from Cr, Re and Mn each having mass fractional purity of 99.99 %. The alloys were separately sealed into quartz ampoules and annealed in an ultra-high purity argon atmosphere at 1343 K for seven days and quenched into iced water. The elemental composition and homogeneity were determined using electron microprobe analyses. The crystal structure was confirmed using X-ray diffraction (XRD). Electrical resistivity (ρ) was measured above 300 K using resistive heating in an inert atmosphere using the standard dc four-probe method and current reversal with Keithley instrumentation. Magnetic susceptibility (χ) was measured using a SQUID-type vibrating sample magnetometer (VSM) MPMS3 of Quantum Design [13]. $\chi(T)$ curves of the $(\text{Cr}_{84}\text{Re}_{16})_{100-y}\text{Mn}_y$ alloy system in a constant applied field (100 Oe) was obtained on increasing T after zero field cooling (ZFC). Measurements were then also done on heating after field cooling (FC) at 100 Oe.

3. Results and discussion

Figures 1(a) and 1(b) show the representative XRD patterns for the $(\text{Cr}_{84}\text{Re}_{16})_{99.7}\text{Mn}_{0.3}$ and $(\text{Cr}_{84}\text{Re}_{16})_{96.9}\text{Mn}_{3.1}$ alloys using with Cu radiation (0.154 nm wavelength). The four characteristic peaks displayed in the XRD patterns confirm the expected body centred cubic (bcc) crystal structure for these alloys.

Measuring the temperature dependence of resistivity (ρ) is a well-established method in locating T_N [11]. The increase in ρ below T_N is due to electron-hole condensation in the nesting octahedra [11] leading to a change in the number of charge carriers available for conduction. As the temperature decreases, the condensation process progresses and there is a decrease in the final density of states. This leads to a decrease in intraband (between nesting octahedra) and interband (between octahedra and reservoir) scattering by impurity atoms which in turn decrease the contribution to resistivity [11]. Addition of Re to Cr, like Mn, increases the electron concentration and T_N [11]. As the spin-glass state is observed as a result of competing magnetic orders, it was necessary to first identify T_N to ensure that

the trends observed in the magnetic susceptibility curves correspond to the antiferromagnetic state of the alloys.

Representative $\rho(T)$ curves for the $(\text{Cr}_{84}\text{Re}_{16})_{100-y}\text{Mn}_y$ alloys with $y = 0.3, 0.4$ and 3.1 , are shown in figure 2. The temperature associated with the minimum in $d\rho(T)/dT$ accompanying the $\rho(T)$ magnetic anomaly is defined as T_N [11]. In general, the size of the anomaly decreases but T_N increases with increase in Mn concentration as expected.

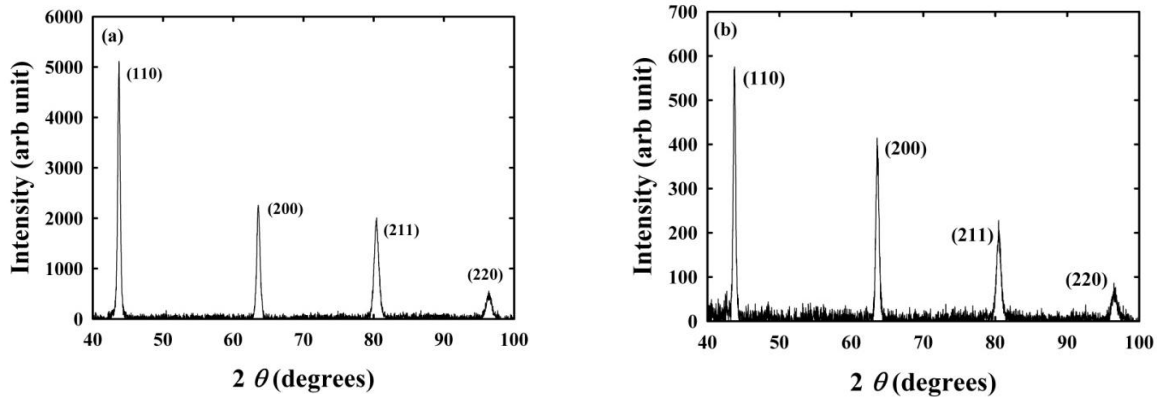


Figure 1: The XRD patterns for (a) $(\text{Cr}_{84}\text{Re}_{16})_{99.7}\text{Mn}_{0.3}$ sample and (b) $(\text{Cr}_{84}\text{Re}_{16})_{96.9}\text{Mn}_{3.1}$ with the Bragg peaks indexed.

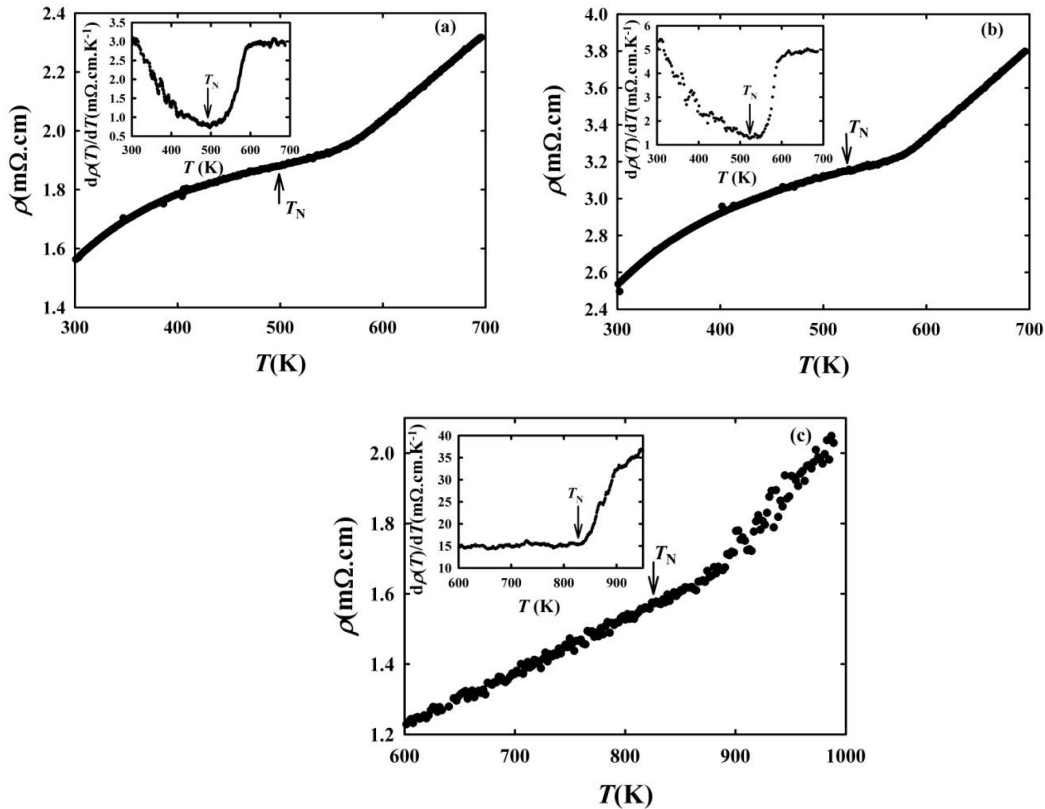


Figure 2: The $\rho(T)$ curves for the $(\text{Cr}_{84}\text{Re}_{16})_{100-y}\text{Mn}_y$ alloy system with, with (a) $y = 0.3$, (b) $y = 0.4$ and (c) $y = 3.1$. The arrow indicates the position of T_N for each alloy. Inset shows the temperature dependence of $d\rho(T)/dT$ with T_N marked at the minimum.

The temperature dependence of magnetic susceptibility (χ) for the alloys with $y = 0.4, 0.6, 0.8$ and 3.1 at.% Mn are shown in figure 3. At low temperatures ($T < 10$ K), a sharp increase in χ is observed on increasing T after ZFC. A prominent peak is observed close to 30 K beyond which χ rapidly decreases to lower values. In samples with concentrations 0.6, 0.8 and 3.1 at.% Mn, χ approaches zero above 40K. In the FC state, there is a slower decrease in χ on increasing T up to around 30 K beyond which the behaviour is identical to that observed in the ZFC state except for the alloy with 3.1 at. % Mn. In this case, the χ values obtained in both the FC and ZFC state first increases to a maximum value resulting in a peak before rapidly decreasing to low χ values. These results are similar to those observed in $\text{Cr}_{1-x}\text{Mn}_x$ alloys [8]. Here too, it is possible to define clearly a “pinning temperature” (T_p) to characterize the onset of the peak. It is important to note that T_p as well as the temperature of the peak show no variation with y . Also, above T_p , χ shows no dependence on temperature up to 400 K. The peak in the temperature dependence of χ with irreversibility with respect to FC and ZFC, the invariance of T_p with y and the invariance of χ with T above T_p are all indicators of this peculiar spin-glass state [8].

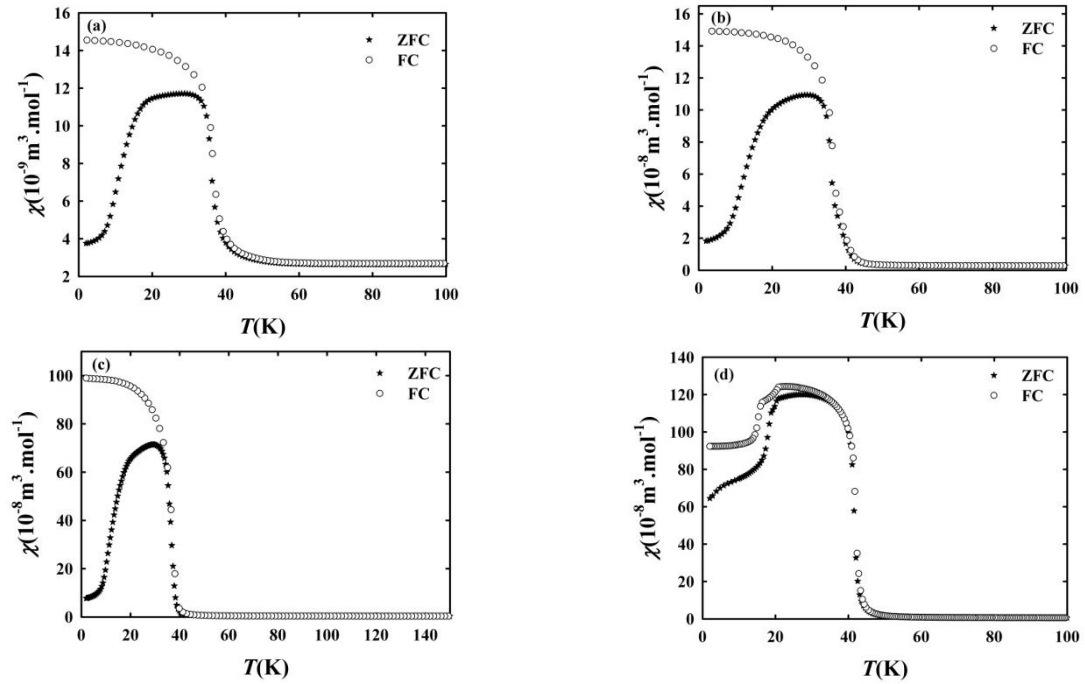


Figure 3. The temperature dependence of χ for the (a) $y = 0.4$ (b) $y = 0.6$ (c) $y = 0.8$ and (d) $y = 3.1$ alloys.

The new type of spin-glass effect found previously in $\text{Cr}_{1-x}\text{Mn}_x$ and $(\text{Cr} + 1.3\% \text{Si})_{1-x}\text{Mn}_x$ [7] is also found in $(\text{Cr}_{84}\text{Re}_{16})_{100-y}\text{Mn}_y$ alloys. The essence of this new type of spin-glass is the frustration of itinerant spins at the interfaces between AFM domains established around each Mn local magnetic moment [11]. Above T_p of the Mn magnetic moments, they follow the AFM domains of the AFM matrix. However, below T_p , the Mn moment is frozen and the AFM order has to follow it, becoming frustrated whenever it finds another fixed moment not pointing in the expected state. This approach supposes that below certain concentration of Mn, the interaction that determines the spin-glass state is at the boundaries of the AF SDW domains, resulting in a peculiar spin-glass that requires the existence of itinerant AFM matrix, contrasting with the canonical spin-glass of CuMn [14]. This is similar to the results reported by Li *et al.* [10] where the sharp downturn of the ZFC M - T curves is an indication of entry into the spin glass or spin frustration state having demagnetizing ferromagnetic domains that

are frozen below T_p and free to rotate above T_p . Figure 3 presents evidence of this behaviour where the pinning temperature does not depend linearly on Mn concentration below the expected incommensurate-commensurate transition for CrMn and CrRe. There is a strong increase of the magnetisation as a function of temperature for commensurate magnetic order.

4. Conclusion

The present study was a preliminary investigation of the electronic and magnetic properties of the $(\text{Cr}_{84}\text{Re}_{16})_{100-y}\text{Mn}_y$ alloy system. Increasing the concentration of Mn leads to increase in T_N as expected. Magnetic susceptibility curves indicate the presence of a possible spin-glass state in the $(\text{Cr}_{84}\text{Re}_{16})_{100-y}\text{Mn}_y$ system requiring the existence of itinerant AFM matrix which is different from that in the canonical CuMn alloy. Results need to be extended to include the tests for spin glass in order to confirm its presence.

Acknowledgements

This work was financially supported by the NRF of South Africa under Grants 80928, 80631, 93551, 80626 and the Faculty of Science at the University of Johannesburg.

References

- [1] Fawcett E 1988 *Rev. Mod. Phys.* **60** 209-283
- [2] Lomer WH 1962 *Proc. Phys. Soc.* **80** 489-496
- [3] Alberts HL 1988 *South African Journal of Science* **84** 32-34
- [4] Alberts HL and Lourens JAJ 1989 *South African Journal of Science* **85** 53-59
- [5] Mydosh JA 1993 "Spin Glasses : An Experimental Introduction" ISBN 0-7484-0038-9 Taylor & Francis London, Washington DC
- [6] Binder K and Young AP 1986 *Rev. Mod. Phys.* **58** 801-976
- [7] Galkin VY, de Camargo PC, Ali N, Schaf J and Fawcett E 1995 *J. Phys. Condens Matter* **7** L649
- [8] Galkin VY, de Camargo PC, Ali N and Fawcett E 1996 *J. Phys. Condens Matter* **8** 7925
- [9] Galkin VY, de Camargo PC, Ali N and Fawcett E 1997 *Physica B* **237-238** 443
- [10] Li B, Alberts HL, Wu BM, Prinsloo ARE and ZJ Chen 2009 *J. Magn. Magn. Mater.* **321** 61-73
- [11] Fawcett E, Alberts HL, Galkin VY, Noakes DR and Yakhmi JV 1994 *Rev. Mod. Phys.* **66** 25-127
- [12] Jacobs BS, Prinsloo ARE, Sheppard CJ and Strydom AM 2013 *J. Appl. Phys.* **113** 17E126
- [13] Quantum Design Inc, 6325 Lusk Boulevard, San Diego, USA
- [14] Retat I and Schwink Ch. 1983 *J. Magn. Magn. Mat.* **38** 123-132